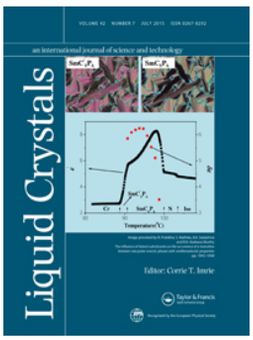

Liquid Crystals

ISSN: 0267-8292 (Print) 1366-5855 (Online) Journal homepage: http://www.tandfonline.com/loi/tlct20

Induced cholesteric solutions of highly soluble bis-salicylaldiminate Cu(II) metallomesogens and their rheological behaviour

Fabio Borbone, Nino Grizzuti, Rossana Pasquino, Laura Ricciotti, Antonio Roviello & Giuseppina Roviello

To cite this article: Fabio Borbone, Nino Grizzuti, Rossana Pasquino, Laura Ricciotti, Antonio Roviello & Giuseppina Roviello (2015) Induced cholesteric solutions of highly soluble bis-salicylaldiminate Cu(II) metallomesogens and their rheological behaviour, Liquid Crystals, 42:7, 1003-1012, DOI: 10.1080/02678292.2015.1013069

To link to this article: http://dx.doi.org/10.1080/02678292.2015.1013069

Liquid Crystals, 2015
Vol. 42, No. 7, 1003–1012, http://dx.doi.org/10.1080/02678292.2015.1013069

Taylor & Francis
Taylor & Francis Group

Induced cholesteric solutions of highly soluble bis-salicylaldiminate Cu(II) metallomesogens and their rheological behaviour

Fabio Borbone[a]*, Nino Grizzuti[b], Rossana Pasquino[b], Laura Ricciotti[c], Antonio Roviello[a] and Giuseppina Roviello[c]

[a]*Dipartimento di Scienze Chimiche, Università degli Studi di Napoli Federico II, Complesso Universitario Monte S. Angelo, Napoli, Italy;* [b]*Dipartimento di Ingegneria chimica, dei Materiali e della Produzione industriale, Università degli Studi di Napoli Federico II, Napoli, Italy;* [c]*Dipartimento di Ingegneria, Università di Napoli Parthenope, Centro Direzionale, 80143 Napoli, Italy*

(*Received 3 December 2014; accepted 26 January 2015*)

Copper(II) complexes containing chiral centres and functionalised with citronellyl end groups were synthesised. Isomerisation of citronellyl double bond was exploited to decrease the melting temperature of the complexes and improve their solubility in organic media. The chiral metallomesogens were successfully used to produce induced cholesteric solutions in commercial nematic liquid crystals also in high concentrations. Transparent and coloured thin films were easily obtained showing good reflective properties across the visible spectrum. The rheological behaviour of the nematic and the cholesteric phases was investigated. The nematic system showed the characteristics of a tumbling phase with a very peculiar transient behaviour. The cholesteric samples also showed a very unusual, flow-history-dependent transient behaviour. The viscosity trend presumably indicates a flow-induced orientation of the cholesteric superstructure, thus opening the way to the possibility of tuning the yield stress level of the material. The results support the potentiality of these compounds for applications in light reflecting technology.

Keywords: cholesteric; metallomesogen; rheology; copper; citronellyl

Introduction

It is well known that chiral liquid crystals (LCs) or LCs containing chiral compounds can generate a cholesteric liquid crystalline (CLC) phase.[1–7] CLCs are characterised by a macroscopically ordered chiral structure where the molecules are organised in nematic layers, whose director orientation varies periodically along the direction perpendicular to the planes. The rotation of the director produces a right-handed or left-handed helix. When the helix axis is perpendicular to the surfaces of the cell containing the cholesteric phase, defect-free, planar or Grandjean textures can be produced.[3] Thin films of this phase appear uniformly transparent and reflect brilliant colours, whose wavelengths depend upon the helical pitch. This effect is due to the periodic helical structure acting as a normal diffraction grating [8] and is responsible for the selective Bragg reflection of the circularly polarised component of the light of the same handedness as the CLC phase. On the contrary, the component with opposite handedness is simply transmitted through the sample. The dependence of the reflected wavelength λ_0 on the helical pitch (p) is given by $\lambda_0 = np$, where n is the average between ordinary (n_o) and extraordinary (n_e) refractive indexes. The reflection peak appears as a band whose width depends on the birefringence of the sample Δn according to the equation $\Delta\lambda = p\Delta n$. This phenomenon can be exploited in the field of display technology as reflection-type LC displays,[9–13] or in polarisers, filters,[14] lasers,[15] smart windows,[16] shutters [17] and solar concentrators.[18] For the same reasons, the CLC property to change colour with temperature [19,20] or substrate bending [21] can also be exploited.

As mentioned earlier, a CLC can be obtained by a pure compound with a chiral centre or by a solution of even small quantities of chiral molecules dissolved in a nematic LC. Within the latter category, low molecular weight chiral molecules containing coordinated transition metals (metallomesogens), which can generate CLC mesophases, are already known in the literature.[22,23] It was recently reported [21] that bis-salicylaldiminate metallomesogens containing Cu(II), Ni(II), Pd(II), vanadyl and their mixtures showed cholesteric phases and were able to reflect a wavelength band when arranged in thin liquid films. A thermal dependence of the pitch was observed for complexes characterised by a temperature-dependent coordination geometry, such as Ni(II) and vanadyl. The use of such metal complexes can be advantageous for applications due to the stabilisation effect of the

*Corresponding author. Email: fabio.borbone@unina.it
Dedicated to Giovanni Romeo

metal coordination and the consequent improvement of chemical and thermal stability.[24–28]

Room temperature CLC liquids could be more attractive for applications than the aforementioned high melting solid complexes or their mixtures. Hence, the possibility to dissolve these compounds in a commercial nematic LC to obtain CLC phases is very attractive. The nematic LC is usually a mixture of organic compounds with low polarity and poor solvent power towards many chiral organic compounds. Moreover, the addition of a further compound can cause excessive decrease of the isotropisation temperature and make the mixture unsuitable for applications. In this work, the chiral Cu(II) complexes previously reported were modified with citronellyl chains with the aim to obtain low melting metallomesogens with high solubility in nematic LCs. Different preparation pathways were also investigated, which affected the melting temperature of the final complex. The CLC solutions showed selective reflection of light, and the reflected wavelength band was tuned from ultraviolet (UV)–visible to near infrared (NIR) by changing the metallomesogen concentration. An investigation of the rheological properties of both the nematic and cholesteric phases was also performed, which showed interesting results. A tumbling nematic response was recorded in the case of the pure commercial nematic used, while the cholesteric phase appeared to be extremely shear thinning with no dependence of the rehological response on the helical handedness.

Experimental

Methods

All solvents and reagents were purchased from Aldrich (Sigma-Aldrich, St. Louis, MO, USA) and used without further purification. ^{1}H Nuclear Magnetic Resonance (NMR) spectra were recorded with a Varian XL 200-MHz (Varian Inc., Palo Alto, CA, USA) apparatus. UV/visible spectra were recorded with a Jasco V560 (Jasco Inc., Easton, MD, USA) spectrophotometer. Thermogravimetric analyses were performed on a TA Instruments (New Castle, DE, USA) SDT 2960 under air flow at 10°C/min. Differential scanning calorimetry (DSC) measurements were performed on a Perkin Elmer (Waltham, MA, USA) Pyris 1 under dry nitrogen flow with a temperature scanning rate of 10°C/min. Optical observations were performed with a Zeiss (Jena, Germany) Axioscop polarising microscope equipped with an FP90 Mettler (Toledo, Greifensee, Switzerland) hot stage. Rheological measurements were performed on a strain controller rheometer (ARES, TA instruments) equipped with either a 200- or a 2000-g cm transducer. A stainless steel cone and plate fixture was used to ensure a constant shear strain throughout the sample (0.02 rad, diameter 50 mm). Temperature of 25°C was controlled via a convection oven, with an accuracy of ±0.1°C. A fully filled cone and plate fixture contains about 1 ml fluid volume. Linear and nonlinear rheological tests have been performed on the nematic samples and on the cholesteric LCs. The linear tests usually consist in dynamic experiments in which the viscoelastic response is analysed by varying the frequency of observation. The nonlinear experiments consist of flow start-up measurements, in which the sample is subjected to a constant shear rate and the apparent viscosity is monitored as function of time.

Synthesis

4-(3,7-Dimethyloct-6-enyloxy)benzoic acid and 4-(3,7-dimethyloct-7-enyloxy)benzoic acid mixture (a)

Citronellol (40 mL) was refluxed in thionyl chloride (60 mL) for 30 minutes. The thionyl chloride was removed and the residue distilled in vacuum. The obtained product (19.16 g), methyl 4-hydroxybenzoate (15.98 g) and potassium carbonate (31.91 g) were added to 100 mL *N*,*N*-dimethylformamide (DMF) and refluxed for 9 h under stirring. The solid was then filtered, the liquid was poured into 500 mL water, and the pH was corrected to 5–6 with acetic acid. The solution was extracted with chloroform (3 × 100 mL), then the organic phases were collected and the solvent removed. The residue was dissolved in 200 mL ethanol, 35 g potassium hydroxide in 100 mL water was added, and the mixture was refluxed for 45 minutes. The product was precipitated through the addition of hydrochloric acid, filtered and recrystallised by ethanol/water.

^{1}H NMR ($CDCl_3$, 200 MHz), δ (ppm): 0.95 (d, 3H); 1.24 (t, 2H); 1.60 (s, 3H); 1.68 (s, 3H); 1.99 (m, 2H); 4.05 (t, 2H); 5.09 (t, 1H); 6.92 (d, 2H); 8.04 (d, 2H).

Citronellyl iodide

Triphenylphosphine (6.15 g, 23.0 mmol), imidazole (1.56 g, 23.0 mmol) and iodine (5.60 g, 22.0 mmol) were added in the order to a solution of β-citronellol (3.00 g, 19.2 mmol) in 40 mL dichloromethane at 0°C. After stirring for 1 h, the reaction mixture was allowed to warm to room temperature over 1 h, before the addition of 7 mL saturated $Na_2SO_{3(aq)}$. The organics were then concentrated by evaporation, and the mixture was taken up in 100 mL hexane, washed with 3 × 40 mL water, dried over Na_2SO_4 and passed through a 2-cm silica gel plug. The organics were concentrated by evaporation to give a light yellow oil (4.20 g, 82% yield).

^{1}H NMR ($CDCl_3$, 200 MHz), δ (ppm): 0.88 (d, 3H); 1.25 (m, 2H); 1.55 (s, 1H); 1.60 (s, 3H); 1.68 (s, 3H); 1.86 (m, 2H); 1.95 (m, 2H); 3.2 (t, 2H); 5.08 (t, 1H).

CL2 (b)

Compound ***a*** (26.8 g), 2,4-diydroxybenzaldehyde (16.1 g) and 4-pyrrolidinopyridine (1.10 g) were dissolved in 210 mL anhydrous tetrahydrofuran (THF). *N*,*N*'-Dicyclohexylcarbodiimide (DCC) (22.0 g) in 50 mL anhydrous THF was slowly added under stirring. After 2 h at room temperature the solid was filtered and 21.3 g copper(II) acetate dissolved in 650 mL ethanol was added to the solution. Sodium acetate (16.0 g) in 150 mL water was slowly added. The solid was filtered, washed twice with water and twice with ethanol. The product was dissolved in 500 mL chloroform and dried over sodium sulphate, and the volume was reduced to about 150 mL. The complex was recrystallised by the addition of 250 mL ethanol.

Aldehydic ligand

The aldehydic ligand was isolated from aldehydic Cu(II) complex. The complex was dissolved in chloroform and 37% wt. HCl was added dropwise under vigorous stirring. The solution colour changed from deep green to yellow, the organic layer was separated, washed several times with water and dried over sodium sulphate, and the solvent was removed by evaporation. A yellow product was obtained.

^{1}H NMR ($CDCl_3$, 200 MHz), δ (ppm): 0.93 (d, 3H); 1.21 (t, 2H); 1.59 (s, 3H); 1.67 (s, 3H); 1.99 (m, 2H); 4.09 (t, 2H); 5.08 (t, 1H); 6.85 (s, 1H); 6.94 (m, 3H); 7.58 (d, 1H); 8.09 (d, 2H); 9.86 (s, 1H); 11.22 (s, 1H).

CR2

Complex ***b*** (4.00 g) and R-(−)-1-amino-2-propanol (0.720 g) were dissolved in 90 mL boiling chloroform. After 5 minutes 7.7 mL hexanoic anhydride were added, and the boiling solution was stirred for 20 minutes. After evaporation of the solvent, 240 mL ethanol was added, the solution was stirred at room temperature for 2 h and left at −15°C for the night. The product was filtered and purified by chromatography (chloroform/hexane 50/50, Florisil 60–100).

The same procedure was applied for the synthesis of complex CS2 by using S-(+)-1-amino-2-propanol.

Results and discussion

The structure of synthesised metallomesogens is reported in Figure 1. A functionalisation with a citronellyl end group was chosen in order to obtain complexes with low melting temperatures and good solubility in common nematic LCs. According to a known procedure,[29] the synthesis was performed through (1) the alkylation of 4-methoxyphenol with the proper citronellyl derivative (see later), (2) the transformation into the corresponding acyl chloride and then (3) the reaction with 2,4-dihydroxybenzaldehyde to give a mixture of isomers. The 4-substituted salicylaldehyde ligand was isolated through *in situ* complexation with Cu(II). The obtained achiral complex **CL2** was converted into two chiral bis-salicylaldiminate complexes by reaction with (S)-(+)- or (R)-(−)-1-amino-2-propanol, whose terminal hydroxyl group was then functionalised by reaction with hexanoic anhydride to further decrease the melting temperature of the complexes (**CS2** and **CR2**, respectively) and improve solubility. The complexation of a divalent metal ion as Cu(II) with a bidentate chiral ligand leads to a molecule with two chiral centres with respect to the free ligand. This approach can be exploited to develop efficient chiral metallomesogens with improved stability that can be used to generate

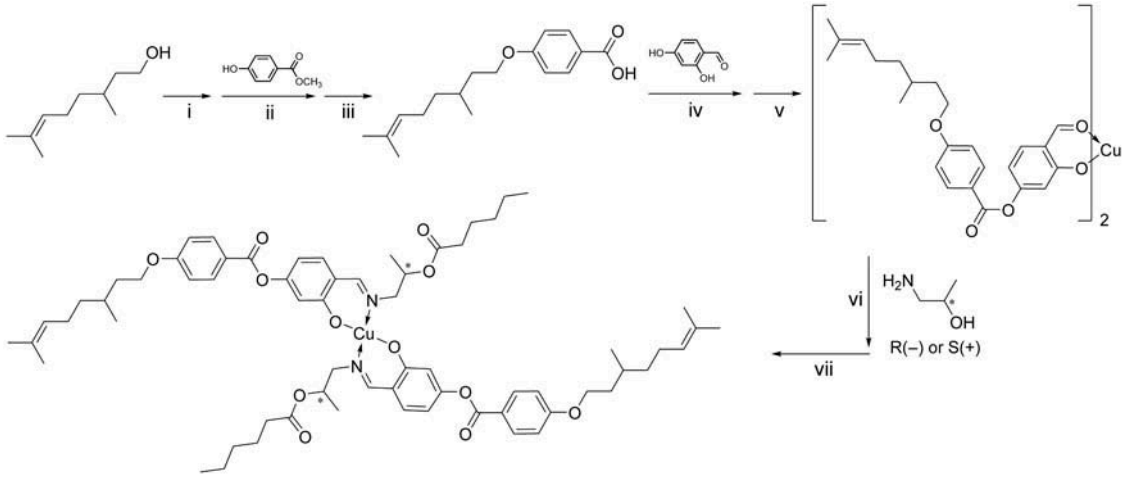

Figure 1. Synthesis scheme of complexes **CS2** and **CR2**. (i) $SOCl_2$, reflux; (ii) K_2CO_3, DMF, reflux; (iii) KOH, boiling EtOH/H_2O; (iv) DCC, PPy, THF; (v) $CuAc_2$, EtOH, H_2O; (vi) (R)/(S)-1-amino-2-propanol, $CHCl_3$; (vii) hexanoic anhydride.

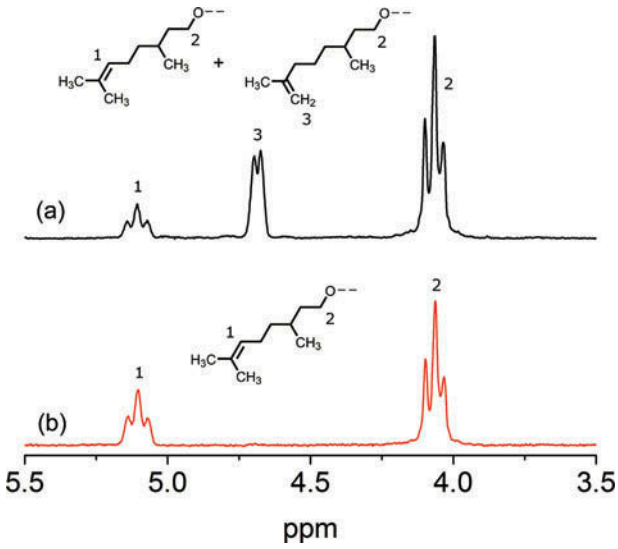

Figure 2. (colour online) ^{1}H NMR spectra of the alkylated 4-hydroxybenzoic acid according to the iodide path (b) and the chloride path (a).

helically structured LC materials for optical application. One of the advantages of this approach is the use of chiral precursors both commercially available and at reasonable and similar cost.

The alkylation with the citronellyl group was performed following two synthetic paths. In the first path β-citronellyl iodide was first obtained by reaction between β-citronellol and iodine in the presence of triphenylphosphine and imidazole under very mild condition (0°C for 1 h, see Experimental section). This reaction selectively produced β-cytronellyl iodide derivative which was then reacted with methyl 4-hydroxybenzoate. The double bond of citronellyl group was preserved as confirmed by the ^{1}H NMR spectrum (reported in Figure 2). This synthetic path produced complexes with a melting point of 81°C and an excellent solubility in organic solvents.

In the second path citronellol was treated with thionyl chloride to obtain the corresponding chloride, which was used for alkylation of methyl 4-hydroxybenzoate. The ^{1}H NMR analysis of the alkylated acid after hydrolysis of the ester revealed the presence of a mixture of isomers, one of them showing the citronellyl double bond in the terminal position (Figure 2). This result was ascribed to the hydrochlorination of citronellol double bond caused by the hydrochloric acid produced during treatment with thionyl chloride and evidenced in the ^{1}H NMR of product by disappearance of CH = resonance at about 5.1 ppm. The addition of chlorine is mainly onto the most substituted (tertiary) carbon according to the Markovnikov rule, leading to a dichloride product. The subsequent alkylation onto the phenolic hydroxyl involved exclusively the primary chlorinated carbon, that is the one with less steric hindrance. The subsequent hydrolysis of the ester in strong basic conditions led to dehydrochlorination and restoration of the double bond on the remaining end, either on the original (citronellyl) or on the new terminal position (Figure 2(a)).

Figure 2 shows a detail of the comparison between the ^{1}H NMR spectrum of the alkylated 4-hydroxybenzoic acid produced according to the iodide path (*b*) and the chloride path (*a*). This region of the spectrum is very informative and clearly shows that the additional signal at 4.7 ppm (typical of terminal alkenes) is only showed in the product of the chloride path. A 50:50 mixture of isomers was obtained with the integration ratio of signals 1, 3, 2 equal to 1:2:4. The double bond isomerism on the substituted benzoic acid led to a consequent ligand isomerism. The complexes obtained by this precursor showed the same chiral behaviour as the complexes with a pure citronellyl end group but a further decrease of the melting temperature was recorded, due to the three possible isomers deriving from copper bis-chelation (DSC analysis, Table 1). Also a better solubility in organic solvents was evidenced. On the basis of these considerations the second synthetic path was used which was also easier and more cost-effective.

The chiral complexes also showed high thermal stability, as demonstrated by decomposition temperatures evaluated by thermogravimetric analysis (Table 1). By this technique the residue of decomposition in air (CuO) was evaluated and confirmed the calculated value of metal content. Besides, the insertion of the lateral chains by formation of coordinated imine led to a sensible increase of the thermal stability with respect to the aldehydic complex and to a strong decrease of the melting points, as it can be evidenced by DSC analysis (Table 1).

Solutions of complexes **CR2** and **CS2** in a commercial nematic LC were prepared in order to evaluate their mesogenic behaviour. The LC TN10427 by Hoffmann La Roche has a high stability range of the

Table 1. Thermal data of complexes.

	T_f[a] (°C)	T_d[b] (°C)	%MO_{calc}[c]	%MO_{exp}[d]
CL2	150	244	9.31	9.26
CR2	71	263	6.83	6.75
CS2	71	280	6.83	6.79

Notes: [a]Melting temperature; [b]decomposition temperature (measured at 5% weight loss); [c]calculated metal content as CuO; [d]experimental metal content as CuO.

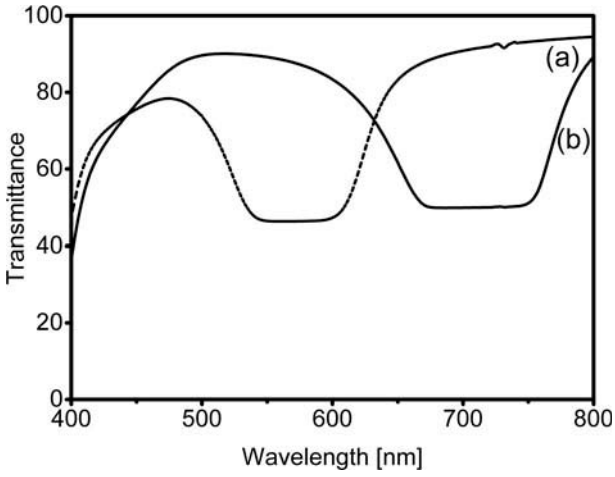

Figure 3. UV–visible spectra of solutions **S16** (a, dashed line) and **S13** (b, solid line).

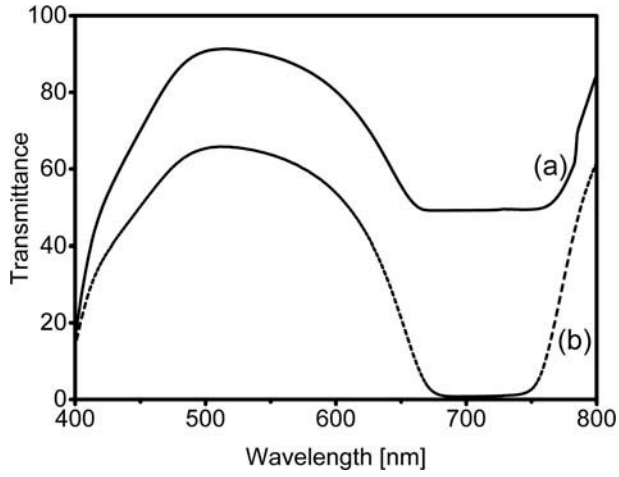

Figure 4. UV–visible spectra of a double layer of **R13** (a, solid line) and a double layer of **R13** and **S13** (b, dashed line).

nematic phase, a good solvent power on the synthesised complexes and a relatively high isotropisation temperature. Solutions with 20%, 16% and 13% wt. concentration of the complex (**R(S)20**, **R(S)16**, **R(S)13**, respectively) were prepared and characterised. The UV–visible spectrum of a thin film of a solution containing **CS2** isomer in 16% wt. (**S16**) shows a reflection band centred at about 570 nm (curve a in Figure 3). The same behaviour was observed for the solution containing **CR2** isomer (R16), as expected. The transmittance value in this region is about 50% or more, due to the residual absorption of the nematic LC solvent, which is saturated in the UV and whose fading intensity depends on the film thickness.

In the spectrum of **S13** the reflection band appears shifted towards higher wavelengths due to the reduced concentration, leading to a longer pitch of the cholesteric phase (curve b in Figure 3). Also in this case the transmittance value is about 50%. The spectrum of two overlaid films of the same solution (Figure 4) still shows a transmittance of about 50%, while the spectrum of two overlaid films of different solutions (R and S) shows that the transmittance falls to zero. This proves that the filter effect is due to the selective reflection of the two circularly polarised components of the radiation operated by the two layers while the absorption effects become gradually more negligible when moving out of the UV region.

The effect of light reflection of the prepared solutions can be appreciated in Figure 5 where a photograph of the three thin films between glass slides illuminated by white light shows the reflected colours from the most concentrated (blue) to the less concentrated (red) solution. In more diluted solutions a

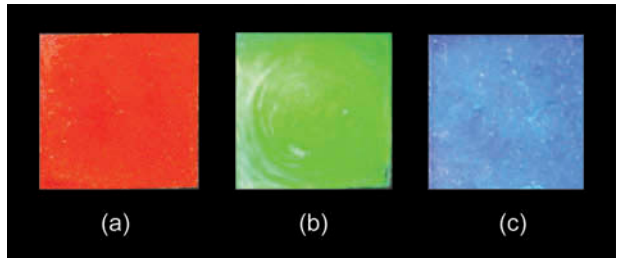

Figure 5. Photograph of **R13** (a), **R16** (b) and **R20** (c) as thin films.

further decrease of the concentration leads to a further shift of the reflection band towards longer wavelengths, which is out of the visible region and in the NIR. The shift from UV to NIR is followed by a broadening of the reflection band.

The helical twisting power (HTP) of the chiral complexes was evaluated by applying the modified 'stripe-wedge' Grandjean–Cano method as reported by Podolsky et al.[30] The HTP is the ability of the chiral molecule to induce helical twisting in the nematic LC and is expressed by the relationship $\beta = (pc)^{-1}$, where c is the concentration of the chiral dopant and p is the cholesteric pitch. The measurement is performed onto thin films of the cholesteric solution and allows for the direct determination of the pitch. For both **CR2** and **CS2** the value of β was 20 μm^{-1}. Finally the helical screw sense of the cholesteric phases was determined according to the Grandjean–Cano method [31] and resulted in right-handed and left-handed sense for **CS2** and **CR2** solutions, respectively.

Rheological characterisation

Nematic sample

The linear viscoelastic response of the nematic sample is shown in Figure 6. A strain amplitude of 20% has been chosen after performing a strain sweep test. The sample has shown to be in the linear regime for strain amplitude lower than 100%. The rheological response is typical of a moderately viscoelastic, nearly Newtonian liquid. On the other hand, a complex transient behaviour is shown in Figure 7, even at shear rates well within the Newtonian plateau. Three different shear rates are considered (10–33–50 s^{-1}) and the apparent viscosity (the stress divided by the shear rate) is plotted as a function of time (Figure 7(a)) and strain (Figure 7(b)). For each experiment a new fresh sample has been loaded. In all cases, at $t = 0$, when the shear rate jumps to the imposed constant value, the apparent viscosity shows several oscillations in time. Their amplitude decreases with increasing strain and eventually disappears.

This response is typical of a tumbling nematic, where the director is forced to rotate by the hydrodynamic torques in a simple shear flow.[32–35] For sufficiently high shear rates, the director starts to rotate through several multiples of π under the influence of the hydrodynamic torque coupled to the director. Correspondingly, the transient shear stress oscillates at the same frequency as the director orientation. Stress maxima and minima follow the same behaviour exhibited by axisymmetric particles in shear flow, a problem first considered and solved by Jeffery.[36] The director orientation tends to increase the elastic energy of the system in the presence of a boundary-induced orientation effect, leading to a decay of the oscillation with shear strain and eventually to a stationary director orientation profile in steady shear flow.[34,35]

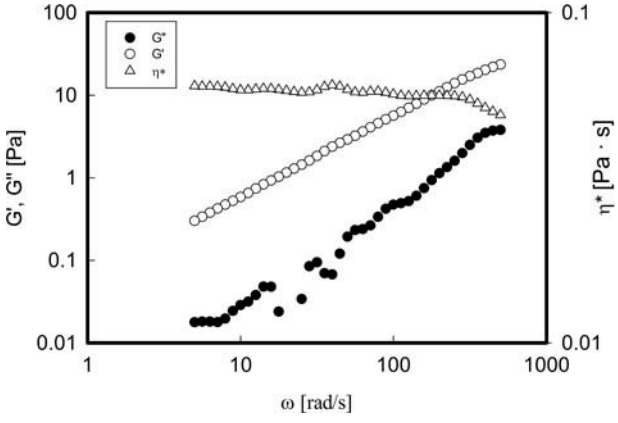

Figure 6. Frequency sweep test for a nematic sample at 25°C with a strain amplitude of 20%.

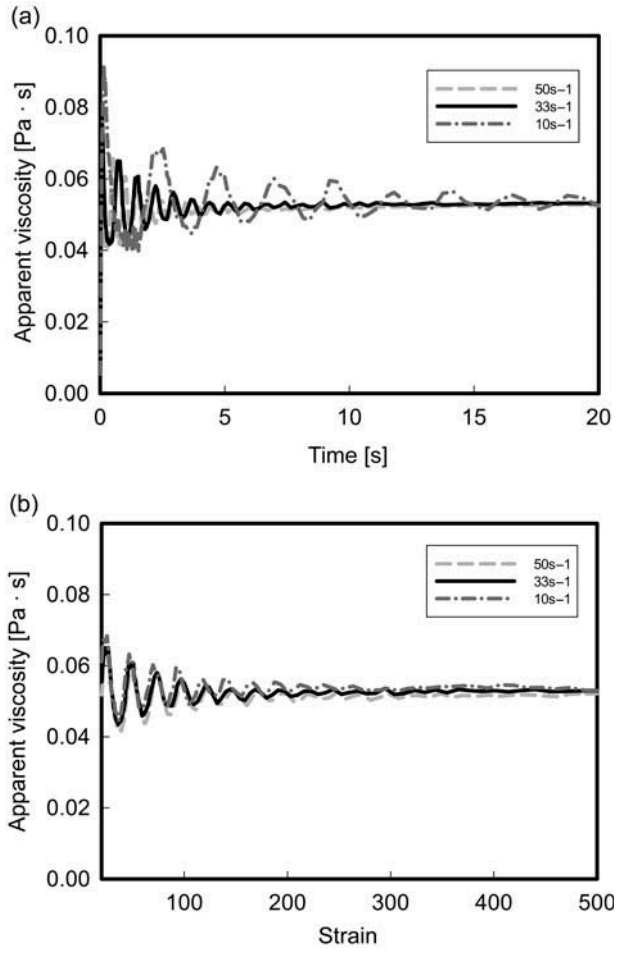

Figure 7. Apparent viscosity as a function of time (a) and strain (b) at 25°C during start-up experiments. Shear rates values are shown in the legend.

The apparent viscosity reaches a stationary value of roughly 52.7(±0.5) mPa · s after about 300 strain units. The major feature of this oscillation response is that the strain periodicity of the oscillations remains constant (24.03 ± 0.9) for different shear rates, suggesting that the tumbling process scales with the shear strain in the range of rates used in our experiments. The scaling suggests that the peaks and the valleys in the stress (and hence viscosity) oscillation correspond to particular director orientation angles. Consequently, the director is rotating with a constant angular velocity. The strain periodicity γ_p of the oscillation can be expressed as [37]

$$\gamma_p = \frac{\pi(1+\delta^2)}{\delta} \tag{1}$$

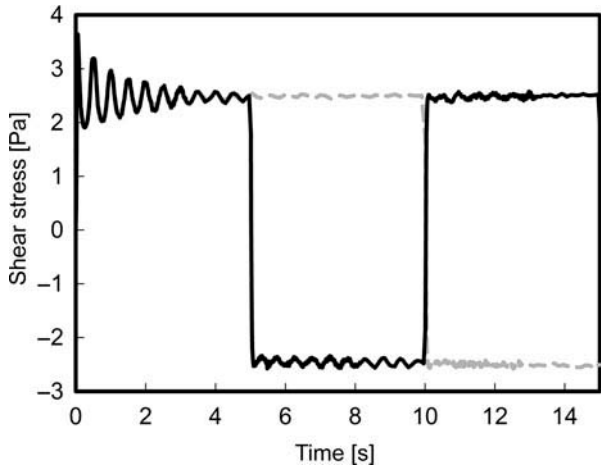

Figure 8. The transient response of the sample to flow reversal (shear rate 50 s^{-1}). Flow is switched at different times during the initial oscillations.

where $\delta = |\alpha_3/\alpha_2|^{0.5}$, with α_2 and α_3 being two of the Leslie viscosity coefficients.[33] It is known that nematics can be divided into two classes according to the sign of the coefficient α_3 (α_2 being always negative). According to the sign of α_3 it is possible to classify the LC in 'flow aligning' ($\alpha_3 > 0$) or 'tumbling' ($\alpha_3 < 0$). According to Equation (1), using the strain periodicity value previously measured ($\gamma_p = 24.03 \pm 0.9$), we obtain $\alpha_3/\alpha_2 = 0.133 \pm 0.005$. This value is in agreement with other literature data, thus indicating that the transient stress response can be well described by Erickson's transversely isotropic fluid model.[38,39]

Figure 8 shows an example of flow reversal experiment in which the nematic sample was subjected to a sudden reversal of the flow direction, at the same shear rate. If flow reversal is applied during the oscillation (black curve), the oscillation continues immediately after the flow reversal. On the other hand, if the flow reversal is applied when oscillations have already disappeared (grey curve), oscillations do not reappear after flow reversal, indicating that the memory of the previous shear history is lost.

Cholesteric samples

The flow behaviour of chiral nematics (or cholesterics) has been little studied.[36,40] Since the cholesteric director varies in a helical fashion, it is impossible to satisfy homeotropic anchoring conditions. Few sets of experiments have demonstrated that the cholesteric phase appears to be extremely shear thinning and perhaps has a yield stress.[41]

Two cholesteric samples were analysed, right-handed **S16** and left-handed **R16** solutions, in cone-plate (50 mm, 0.02 rad) and in parallel plate (25 mm, variable gaps) geometries. Both samples show a very interesting transient flow-history-dependent behaviour.

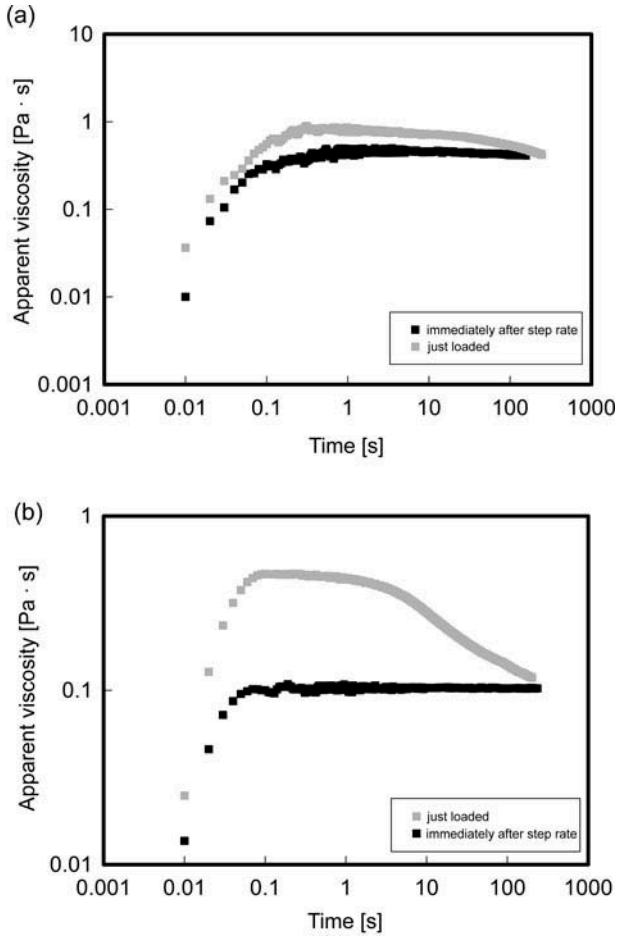

Figure 9. Start-up experiments at 1 s^{-1} (a) and 10 s^{-1} (b). Grey squares refer to a just loaded in cone-plate geometry; black squares refer to a second start-up experiment immediately after the first one. Data are for the left-handed sample but the same response has been found for the other cholesteric director.

Figure 9(a) and (b) shows a start-up experiment for the left-handed sample at two different shear rates, performed with cone-plate geometry. The high viscosity at short times and the subsequent drop (particularly relevant at the higher shear rates), as well as the fact that the phenomenon is not repeated in the second run, can be presumably attributed to the flow-induced orientation of the cholesteric superstructure.[36]

A frequency sweep test has been performed just before and just after the flow start-up experiment. Figure 10 shows the complex viscosity as function of frequency in the two cases. It is clear that the

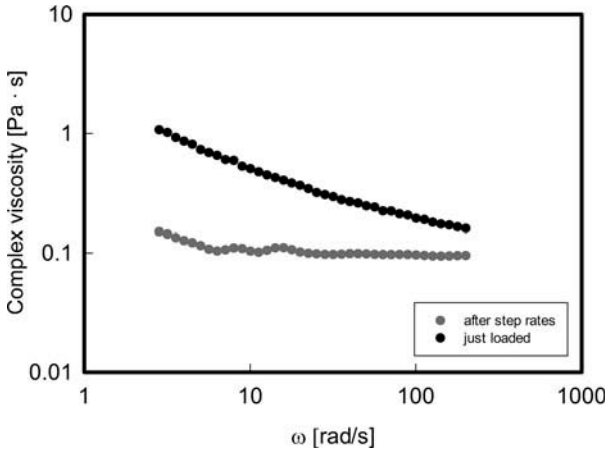

Figure 10. Complex viscosity as a function of frequency for a left-handed cholesteric sample. See text for details.

Bingham-like behaviour of just-loaded sample (with a yield stress of few Pascal) is replaced by a Newtonian behaviour with a much lower viscosity when the frequency sweep is performed at the end of the transient start-up experiment.

The same type of behaviour characterises also the right-handed cholesteric sample if a cone-plate geometry is used.

The geometry seems not to have any influence on the rheological response. Figure 11 shows step rate experiments at varying gap size, shear rate and flow direction with a parallel plate geometry. For a matter of clarity and to show that the response does not change by changing the cholesteric director, the data shown in Figure 11 are for the right-handed cholesteric sample.

The viscosity drops down earlier at higher shear rates, confirming a stronger flow-induced orientation (Figure 11(a)). As already said, the transient behaviour does not seem to be dependent neither on the used geometry nor on the cholesteric director (right-handed or left-handed), and this can be confirmed by comparing Figure 11 with Figure 9. More specifically, Figure 11(b) shows different experiments with variable gap sizes in parallel plate geometry. The apparent viscosity could indeed be sensitive to the cholesteric pitch, which is usually a few microns or less, and to the geometry used for the experiment.[36] We do not see any dependence of the flow response on the gap size (Figure 11(b)). The apparent viscosity could also depend on the winding direction of the cholesteric helix. Clockwise and counterclockwise experiments give the same rheological response with no evidence of dependence upon the helical director pattern (Figure 11(c)).

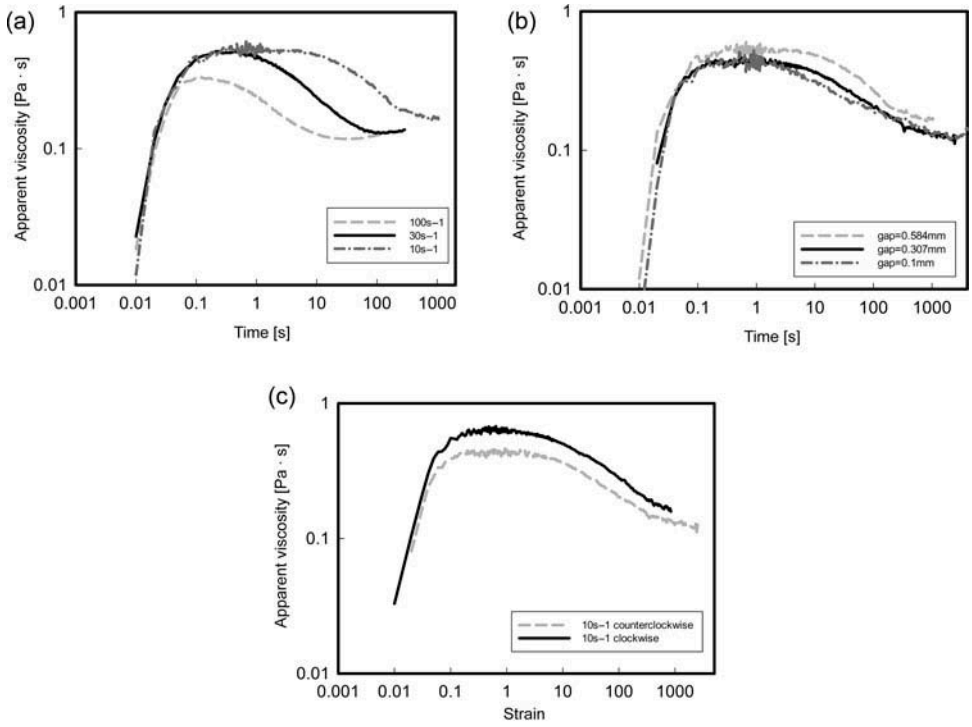

Figure 11. Transient viscosity for the right-handed cholesteric sample. (a) Start-up flow at different shear rates (namely 10–30–100 s^{-1}, gap = 1 mm); (b) start-up flow at 10 s^{-1} at different gaps, using a parallel plate geometry; (c) start-up flow at 10 s^{-1} (gap = 1 mm), in clockwise and counterclockwise directions.

Conclusions

In this work chiral bis-salicylaldiminate Cu(II) complexes were synthesised and functionalised with citronellyl chains to successfully obtain low melting metallomesogens with high solubility in a nematic LC. The low melting temperature of the final complex was further decreased through a synthetic approach which favoured isomerisation of citronellyl double bond to the original and terminal positions. The complexes were successfully used to produce cholesteric solutions which showed selective reflection of light as thin films. The helical pitch and hence the reflected wavelength band was dependent on the metallomesogen concentration. The rheological behaviour of the nematic LC and the cholesteric solutions was carefully investigated, especially during their transient regime. The commercial nematic sample showed a steady-state Newtonian behaviour, but a very peculiar transient response. The latter evidenced the tumbling character of the nematic sample. Tumbling was found to scale with the shear strain in the range of rates used in the experiments. Conversely, the cholesteric samples showed an unusual time-dependent Bingham-like behaviour, with a tunable, flow-history-dependent yield stress. The abrupt decrease of viscosity in the start-up flow is suggestive of a flow-induced orientation of the cholesteric superstructure. The cholesteric director (right-handed or left-handed) and the geometrical flow conditions do not have any influence on the complex rheological response.

Disclosure statement

No potential conflict of interest was reported by the authors.

References

[1] Kelker H, Hatz R. Handbook of liquid crystals. Weinheim: Verlag Chemie; 1990.

[2] Elser W, Ennulat RD. Selective reflection of cholesteric liquid crystals. In: Brown GH, editor. Advances in liquid crystals. Vol. 2. New York (NY): Academic Press; 1976. p. 73–172. doi:10.1016/B978-0-12-025002-8.50009-9

[3] Chilaya GS, Lisetski LN. Cholesteric liquid crystals: physical properties and molecular-statistical theories. Mol Cryst Liq Cryst. 1986;140:243–286. doi:10.1080/00268948608080157

[4] Huang D, Yang J, Wan W, Ding F, Zhang L, Liu Y, Xiang S. Cholesteric metallomesogens containing optically active metal-tricarbony moieties. Mol Cryst Liq Crys A. 1996;281:43–49. doi:10.1080/10587259608042230

[5] Shanker G, Yelamaggad CV. A new class of low molar mass chiral metallomesogens: synthesis and characterization. J Mater Chem. 2011;21:15279–15287. doi:10.1039/c1jm11947h

[6] Baena MJ, Buey J, Espinet P, Kitzerow HS, Heppke G. Metallomesogens with a cholesteric mesophase. Angew Chem Int Edit. 1993;32:1201–1203. doi:10.1002/anie.199312011

[7] Thompson NJ, Serrano JL, Baena MJ, Espinet P. Effect of the position and number of chiral carbons on ferroelectric liquid crystals from multichain mononuclear ortho-palladated complexes. Chem–Eur J. 1996;2:214–220. doi:10.1002/chem.19960020214

[8] Shashidhara Prasad J. On the theories of optical reflection from cholesteric liquid crystal films. In: Johnson J, Porter R, editors. Liquid crystals and ordered fluids, Vol. 2. New York (NY): Springer US; 1974. p. 607–612.

[9] Mitov M. Cholesteric liquid crystals with a broad light reflection band. Adv Mater. 2012;24:6260–6276. doi:10.1002/adma.201202913

[10] White TJ, Bricker RL, Natarajan LV, Tondiglia VP, Green L, Li Q, Bunning TJ. Electrically switchable, photoaddressable cholesteric liquid crystal reflectors. Opt Express. 2010;18:173–178. doi:10.1364/OE.18.000173

[11] Wu ST, Yang DK. Reflective liquid crystal displays. New York (NY): Wiley; 2001.

[12] Yang DK. Flexible bistable cholesteric reflective displays. J Disp Technol. 2006;2:32–37. doi:10.1109/JDT.2005.861595

[13] Tamaoki N. Cholesteric liquid crystals for color information technology. Adv Mater. 2001;13:1135–1147. doi:10.1002/1521-4095(200108)13:15<1135::AID-ADMA1135>3.0.CO;2-S

[14] Broer DJ, Lub J, Mol GN. Wide-band reflective polarizers from cholesteric polymer networks with a pitch gradient. Nature. 1995;378:467–469. doi:10.1038/378467a0

[15] Kopp VI, Fan B, Vithana HKM, Genack AZ. Low-threshold lasing at the edge of a photonic stop band in cholesteric liquid crystals. Opt Lett. 1998;23:1707–1709. doi:10.1364/OL.23.001707

[16] Cupelli D, Nicoletta FP, Manfredi S, Vivacqua M, Formoso P, De Filpo G, Chidichimo G. Self-adjusting smart windows based on polymer-dispersed liquid crystals. Sol Energ Mat Sol C. 2009;93:2008–2012. doi:10.1016/j.solmat.2009.08.002

[17] Kumar R, Raina KK. Electrically modulated fluorescence in optically active polymer stabilised cholesteric liquid crystal shutter. Liq Cryst. 2014;41(2):228–233. doi:10.1080/02678292.2013.851287

[18] Rodarte AL, Cisneros F, Hirst LS, Ghosh S. Dye-integrated cholesteric photonic luminescent solar concentrator. Liq Cryst. 2014;41(10):1442–1447. doi:10.1080/02678292.2014.924163

[19] Hanson H, Dekker AJ, Van Der Woude F. Composition and temperature dependence of the pitch in cholesteric binary mixtures. Mol Cryst Liq Cryst. 1977;42:15–32. doi:10.1080/15421407708084492

[20] Ennulat RD. The selective light reflection by plane textures. Mol Cryst Liq Cryst. 1971;13:337–355. doi:10.1080/15421407108083550

[21] Shibaev PV, Newman L. Remote optical detection of bending deformations by means of cholesteric paint. Liq Cryst. 2013;40(3):428–432. doi:10.1080/02678292.2012.755225

[22] Pyżuk W, Galyametdinov Y. Paramagnetic chiral mesophases of Shiff's base complexes of transition metals. Liq Cryst. 1993;15:265–268. doi:10.1080/02678299308031958

[23] Bacilieri A, Caruso U, Panunzi B, Roviello A, Sirigu A. Cholesteric liquid crystal polymers containing coordinated copper(II) in the main chain. Polymer. 2000;41:6423–6430. doi:10.1016/S0032-3861(99)00898-8
[24] Borbone F, Carella A, Caruso U, Roviello G, Tuzi A, Dardano P, Lettieri S, Maddalena P, Barsella A. Large second-order NLO activity in poly(4-vinylpyridine) grafted with PdII and CuII chromophoric complexes with tridentate bent ligands containing heterocycles. Eur J Inorg Chem. 2008;1846–1853. doi:10.1002/ejic.200701171
[25] D'Auria I, Lamberti M, Mazzeo M, Milione S, Roviello G, Pellecchia C. Coordination chemistry and reactivity of zinc complexes supported by a phosphido pincer ligand. Chem–Eur J. 2012;18:2349–2360. doi:10.1002/chem.201102414
[26] Li G, Lamberti M, Roviello G, Pellecchia C. New titanium and hafnium complexes bearing [−NNN–] pyrrolylpyridylamido ligands as olefin polymerization catalysts. Organometallics. 2012;31:6772–6778. doi:10.1021/om300519s
[27] Borbone F, Caruso U, Centore R, De Maria A, Fort A, Fusco M, Panunzi B, Roviello A, Tuzi A. Second order optical nonlinearities of copper(II) and palladium(II) complexes with N-salicylidene-N′-aroylhydrazine tridentate ligands. Eur J Inorg Chem. 2004;2467–2476. doi:10.1002/ejic.200300735
[28] Borbone F, Caruso U, De Maria A, Fusco M, Panunzi B, Roviello A. (4-Vinylpyridine-styrene) copolymer as host polymer for chromophoric complexes with potential second order nonlinear optical properties. Macromol Symp. 2004;169:313–322. doi:10.1002/masy.200451432
[29] Borbone F, Carella A, Roviello G, Ricciotti L, Panunzi B, Catauro M, Roviello A. Synthesis and thermotropic behavior of cholesteric mixtures containing metallomesogen Cu(II), Ni(II), Pd(II) and vanadyl complexes. Inorg Chem Commun. 2013;38:135–138. doi:10.1016/j.inoche.2013.10.028
[30] Podolsky D, Banji O, Rudquist P. Simple method for accurate measurements of the cholesteric pitch using a "stripe–wedge" Grandjean–Cano cell. Liq Cryst. 2008;35:789–791. doi:10.1080/02678290802175756
[31] Gerber PR. On the determination of the cholesteric screw sense by the Grandjean-Cano method. Z Naturforsch. 1980;35:619–622.
[32] De Gennes PG. The physics of liquid crystals. Oxford: Clarendon; 1974.
[33] Burghardt WR, Fuller GG. Transient shear flow of nematic liquid crystals: manifestations of director tumbling. J Rheol. 1990;34:959–992. doi:10.1122/1.550151
[34] Gu D, Jamieson AM, Wang SQ. Rheological characterization of director tumbling induced in a flow-aligning nematic solvent by dissolution of a side-chain liquid-crystal polymer. J Rheol. 1993;37:985–1001. doi:10.1122/1.550381
[35] Gu D, Jamieson AM. Shear deformation of homeotropic monodomains: temperature dependence of stress response for flow-aligning and tumbling nematics. J Rheol. 1994;38:555–571. doi:10.1122/1.550474
[36] Larson RG. The structure and rheology of complex fluids. New York (NY): Oxford University Press; 1998.
[37] Marrucci G. Rheology of liquid crystalline polymers. Pure Appl Chem. 1985;57:1545–1552. doi:10.1351/pac198557111545
[38] Kneppe H, Schneider F, Sharma NK. A comparative study of the viscosity coefficients of some nematic liquid crystals. Berich Bunsen Gesell. 1981;85:784–789. doi:10.1002/bbpc.19810850810
[39] Kneppe H, Schneider F, Sharma NK. Rotational viscosity γ1 of nematic liquid crystals. J Chem Phys. 1982;77:3203–3208. doi:10.1063/1.444195
[40] Venhaus DG, Conatser KS, Green MJ. Dynamics of chiral liquid crystals under applied shear. Liq Cryst. 2013;40(6):846–853. doi:10.1080/02678292.2013.779037
[41] Sakamoto K, Porter RS, Johnson JF. The Viscosity of mesophases formed by cholesteryl myristate. Mol Cryst. 1969;8:443–455. doi:10.1080/15421406908084920